

## CHARACTERIZATION OF FINE PARTICLES VIA ELLIPTICALLY-POLARIZED LIGHT SCATTERING

**M. Pinar Mengüç, Ph.D.,**  
 Department of Mechanical Engineering  
 University of Kentucky  
 Lexington, KY 40506  
 menguc@enr.uky.edu

### PREFACE

*This short review paper is to give an overview of the particle characterization research carried out at the University of Kentucky during the last decade. This work has been a product of several MS or PhD students, who still continue on advancing the field via their research and development applications. Many different particles have been the focus of our attention, varying from pulverized coal to soot agglomerates, from phytoplankton to cotton fibers, from fat in milk to bubbles in process columns, from foam to metallic nano-colloids. The work has been exciting and rewarding, resulted in several papers, presentations, patents, prototypes. And, all started from that wonderful inspiration I found at the view of reddish/yellowish light scattered by the particles emitted from the Purdue smokestack, long gone from the silhouette of the Purdue campus. Yet, it had a lasting impact!*

### INTRODUCTION

When light, or any electromagnetic wave, is incident on a particle, a surface, or any object, it is absorbed, transmitted, reflected, refracted, and diffracted. These interactions are defined rigorously via Maxwell's equations. If a medium is comprised of several objects, the fate of the incident wave within the medium is determined by considering the cumulative interactions. If a series of assumptions can be made, these relatively complex equations can be replaced with simpler expressions of geometric optics. Using these equations, one can write an expression for the conservation of the radiative energy along a given direction (see Fig. 1). In its simplest form, this equation is the familiar radiative transfer equation, the famous RTE, as can be found in many textbooks or monographs [1-3].

In principle, the RTE represents the change of radiative intensity along a line-of-sight, per unit time, solid angle, and frequency. If we consider a beam of radiation propagating through such a medium in the direction  $\Omega$  (see Fig.1), the intensity at a given location is defined as  $I_\lambda(\Omega)$ . As the beam

moves along, it will lose some of its energy due to absorption and scattering. Mathematically, the reduction of intensity due to absorption and scattering along a distance  $ds$  are proportional to the incident intensity, and can be expressed as  $-\kappa_\lambda I_\lambda(\Omega)ds$  and  $-\sigma_\lambda I_\lambda(\Omega)ds$ , respectively. Here,  $\kappa_\lambda$  is the spectral absorption coefficient and  $\sigma_\lambda$  is the spectral scattering coefficient, with units of inverse distance, i.e.,  $[m^{-1}]$ . The total loss of radiation energy, known as extinction, is the sum of absorption and scattering. The spectral extinction coefficient is expressed as  $\beta_\lambda = \kappa_\lambda + \sigma_\lambda$ . The fraction of attenuated (extinct) energy due to scattering is known as the single scattering albedo:  $\omega_\lambda = \sigma_\lambda/\beta_\lambda$  [1-3].

The absorbed energy is promptly converted to thermal energy (heat). The scattered energy is redistributed throughout the medium. This scattered energy carries the information about the medium, and if it is quantified properly, it may help characterization of the objects in the medium.

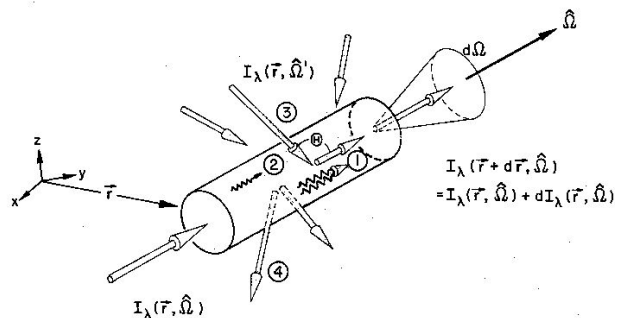


**Fig.1** Schematic to depict the conservation of radiation intensity along a line of sight.

As shown in Fig. 1, absorption (2) and out-scattering (4) account for the losses, and the emission (1) and in-scattering (3) make up the gain terms. Once these terms are tallied, we arrive at the RTE [1-3].

The term “scattering” refers to the combined effect of reflection, refraction and diffraction, and it is basically because of the presence of particles, or any inhomogeneities. If the frequency or the wavelength of radiation does not change via scattering, it is *elastic scattering*. If the frequency shifts during the absorption/re-emission process, then it is referred to as *inelastic scattering*.

The integro-differential form of the RTE is due to the *in-scattering* term. For the solution of the RTE, it is necessary to know how different size and shape particles with different material properties may scatter incident radiation. This information either comes from experiments, or by solving the Maxwell equations, as discussed below, as a function of particle shape, structure, wavelength of the incident radiation, and the dielectric constants of the medium and the particles. The results of these calculations yield absorption and differential cross-section for *single scattering*. In the presence of many particles, the cumulative effect of all need to be considered, which is done by solving the RTE.

If particles are several wavelength away from each other, which is as usually the case for most practical situations, then the single scattering effects can be added linearly (via the in-scattering term), and with this approach the *multiple scattering* can be accounted for in the calculations. It should be understood, however, that there is an implicit approximation made here for multiple scattering calculations. The single-scattering calculations are based on a planar wave being incident on a particle. After scattering, the waves emanated from the particle are spherical, but, as they radiate away they become more planar in shape. If the second particle is several wavelengths away from the scattering center, then the results of single-scattering calculations based on a planar wave are valid, and we can predict the behavior of the scattering by the second particle easily. If the particles closer to each other than two to three wavelengths, or if they are touching each other, then we have to solve more complicated expressions via Maxwell’s equations to account for this *dependent scattering*. In the case of agglomerates of particles, the dependent scattering effects need to be considered as rigorously as possible.

It is obvious that by solving the RTE we will be able to account for the effect of scattering by particles on the scattered intensity distribution outside the boundaries of the medium. This means that if we measure the scattering patterns outside a medium, we should be able to determine the size, shape, and structure of these particles following an inverse radiation analysis. Such an inverse approach requires the availability of an extensive database which documents the scattering patterns of different size and shape of particles with different dielectric constants, or the refractive indices. Therefore, a particle characterization methodology requires first and the foremost, accurate solution algorithms to determine the differential scattering cross-sections of different particles. In the following section, we give an overview of different techniques we have developed and used for this purpose.

The next step is the design of an experimental system to obtain the most information for characterization of particles.

For this purpose, angular profiles of scattered light can be used. However, if elliptically polarized light is employed, more accurate and detailed characterization will be possible. This requires the detection of Stokes parameters as a function of scattering angle, which can be accomplished by using a predetermined set of polarizers and retarders. This approach will allow us to quantify the change in the ellipticity of the polarization of the scattered light, which yield information about the size, shape and structure of particles. Symmetry is always beautiful to observe and simple to use; however, one can obtain much detailed information from asymmetry. The use of asymmetry in elliptically polarized scattering light is the backbone philosophy of our experimental design.

Below, we will first discuss briefly the theoretical and experimental approaches. After that, we will present a series of results for different physical systems and particles.

## SINGLE SCATTERING MODELS

The single scattering problem is expressed as: Given a particle of specified size, shape and material properties that is illuminated by an arbitrarily polarized monochromatic wave, determine the electromagnetic (EM) field at all points within the particle and in the medium in which the particle is embedded. The field inside the particle is denoted by  $(\mathbf{E}_1, \mathbf{H}_1)$ ; the field  $(\mathbf{E}_2, \mathbf{H}_2)$  in the medium surrounding the particle is the superposition of the incident field  $(\mathbf{E}_i, \mathbf{H}_i)$  and the scattered field  $(\mathbf{E}_s, \mathbf{H}_s)$ . (See Figure 2.)

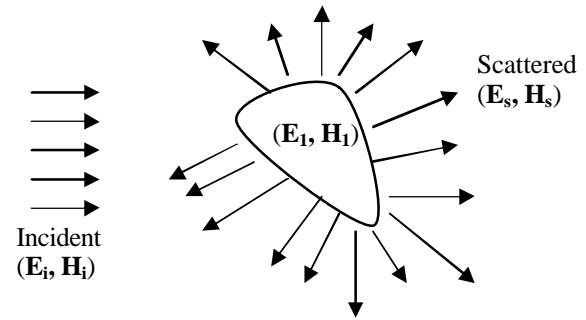


**Fig.2** Scattering of EM-waves by an arbitrarily-shaped particle.

The EM field obeys Maxwell’s equations at all points. Since an arbitrarily polarized wave can be represented by the superposition of two orthogonally polarized plane waves, we need to solve each scattering problem twice, one for the parallel (s) and one for the perpendicular (p) component, in order to determine the scattering patterns. For the analysis, we assume a planar, harmonic wave incident on the particle, which is expressed as

where  $k = 2\pi n/\lambda$  is the wave number,  $n$  is the refractive index, and  $\lambda$  is the wavelength of the incident light in vacuum. At sufficiently large distances from the origin, ( $kr \gg 1$ ), i.e., in the *far-field region*, the scattered electric field  $\mathbf{E}_s$  is approximately *transverse* ( $\hat{\mathbf{e}}_r \cdot \mathbf{E}_s \approx 0$ ) [4]. The relation between incident and scattered fields is conveniently written in matrix form as

$$\begin{pmatrix} E_{//s} \\ E_{\perp s} \end{pmatrix} = \frac{e^{ik(r-z)}}{-ikr} \begin{pmatrix} S_2 & S_3 \\ S_4 & S_1 \end{pmatrix} \begin{pmatrix} E_{//i} \\ E_{\perp i} \end{pmatrix}$$

The elements  $S_j$  ( $j = 1,2,3,4$ ) of the *amplitude scattering matrix* depend, in general, on the zenith angle  $\theta$ , and the azimuthal angle  $\phi$ . The real and imaginary parts of the four amplitude scattering matrix elements can rarely be measured for all values of  $\theta$  and  $\phi$ . It is a very difficult measurement at frequencies corresponding to visible light, which are on the order of  $10^{14}$  Hz. Hence, very few such experiments have been performed. However, the amplitude scattering matrix elements are related to quantities that are much easier to measure than phases.

Once the electromagnetic fields inside and scattered by the particle are obtained, Poynting vector at any point can be determined. The Poynting vector is a measure of the energy flux carried by an electromagnetic wave. It is defined as the cross product of the electric and magnetic field vectors:  $\mathbf{P}=\mathbf{E}\times\mathbf{H}$ . Suppose that a detector is placed at a distance  $\mathbf{r}$  from a scattering particle in the far-field region, with its surface  $\Delta A$  aligned normal to  $\hat{\mathbf{e}}_r$ . The detector records a signal proportional to  $\mathbf{P}_s\cdot\hat{\mathbf{e}}_r\Delta A$ . The detector “sees” only the scattered light provided that it does not “look at” the source of incident light [4].

Now imagine an arbitrarily polarized EM wave. The complete polarization state of the wave is expressed via a column vector of the four Stokes Parameters, where the brackets  $\langle \rangle$  indicate the time average [4,5]:

$$\begin{aligned} I &= \langle E_{//}E_{//}^* + E_{\perp}E_{\perp}^* \rangle \\ Q &= \langle E_{//}E_{//}^* - E_{\perp}E_{\perp}^* \rangle \\ U &= \langle E_{//}E_{\perp}^* + E_{\perp}E_{//}^* \rangle \\ V &= i\langle E_{//}E_{\perp}^* - E_{\perp}E_{//}^* \rangle \end{aligned}$$

These four quantities of the scattered light can be measured by a detector. The Stokes parameters of the incident and scattered beams are related via  $4 \times 4$   $\mathbf{S}$  matrix called the *scattering*, or *Mueller matrix* for a single particle [4,5].

$$\begin{Bmatrix} I_s \\ Q_s \\ U_s \\ V_s \end{Bmatrix} = \frac{1}{k^2 r^2} \begin{pmatrix} S_{11} & S_{12} & S_{13} & S_{14} \\ S_{21} & S_{22} & S_{23} & S_{24} \\ S_{31} & S_{32} & S_{33} & S_{34} \\ S_{41} & S_{42} & S_{43} & S_{44} \end{pmatrix} \begin{Bmatrix} I_i \\ Q_i \\ U_i \\ V_i \end{Bmatrix}$$

The Stokes parameters of the light scattered by a collection of randomly separated particles are the sum of those of the individual particles. Therefore, the scattering matrix for such a collection is merely the sum of the individual particle scattering matrices. Only the seven of the sixteen scattering matrix elements are independent if we have large number of particles in the medium. Measurement of  $S_{11}$ ,  $S_{12}$ ,  $S_{33}$ , and  $S_{34}$  are usually sufficient for characterization of particles with practical interest [6].

The task now is to solve the Maxwell equations to determine the scattering patterns as a function zenith and azimuthal angles, and then to calculate each of the relevant

scattering matrix elements. Finally, using these expressions we determine how much energy would be received by a detector at a given angular location. For an elliptically polarized beam, we will be able to calculate the elliptically polarized scattered intensity incident on a detector. That information, after being corrected for multiple scattering effects, can be used to characterize the size and shape of the particles [6,7].

Below, a series of sample results is outlined in terms of  $S_{ij}$  elements for different shape and structure particles. This information will be needed in the inverse analyses, as it will comprise the database to be used for data reduction after carefully conducted experiments.

### $S_{ij}$ PROFILES FOR DIFFERENT PARTICLES

The solution of the Maxwell equations is necessary to obtain the  $S_{ij}$  elements discussed above. The best known approach for such a solution is the Lorenz-Mie (LM) theory, which was originally developed for homogeneous spherical particles (see [4,5] for detailed reviews of the LM as well as all other techniques we discuss here). Even though the symmetry of a sphere is quite convenient for modeling efforts, most of the practical particles are not spherical, and for advanced characterization as well as material process applications, the asymmetrical nature of scattering objects need to be accounted for in the calculations.

In modeling non-spherical particles, we first need to visualize how they look, and then determine how they would scatter elliptically polarized light. It is intuitive to construct particle shapes and structures following a bottom-up philosophy, as this will allow a more realistic representation of irregular shaped-particles. To this end, we consider small monomers, each with 20-50 nm in diameter, and construct any shape we need to model. This concept was discussed in depth by Manickavasagam and Mengüç [6], where fractal-like soot agglomerates were constructed. A series of sample structures considered for this purpose are depicted in Figure 3.

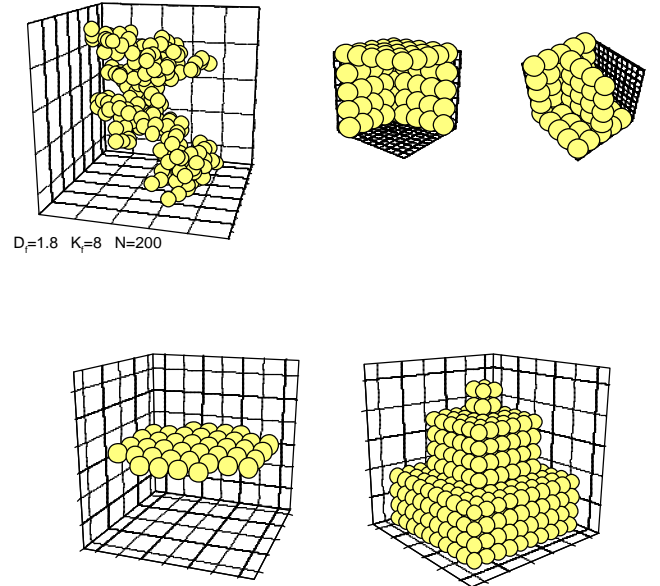


**Fig.3** Different structures modeled using volume integral formulation; each sphere depicts a monomer.

It is important to realize that each monomer that makes up a structure is either touching at least one other, or within a very close proximity of the others. Therefore, straight forward modeling of scattering phenomena as if they are stand-alone, small spherical particles will not produce acceptable results. The dependent scattering effects need to be accounted for in the formulation, as done in discrete-dipole or volume-integral approximations (see references [6,8,9] for the extensive literature reviews).

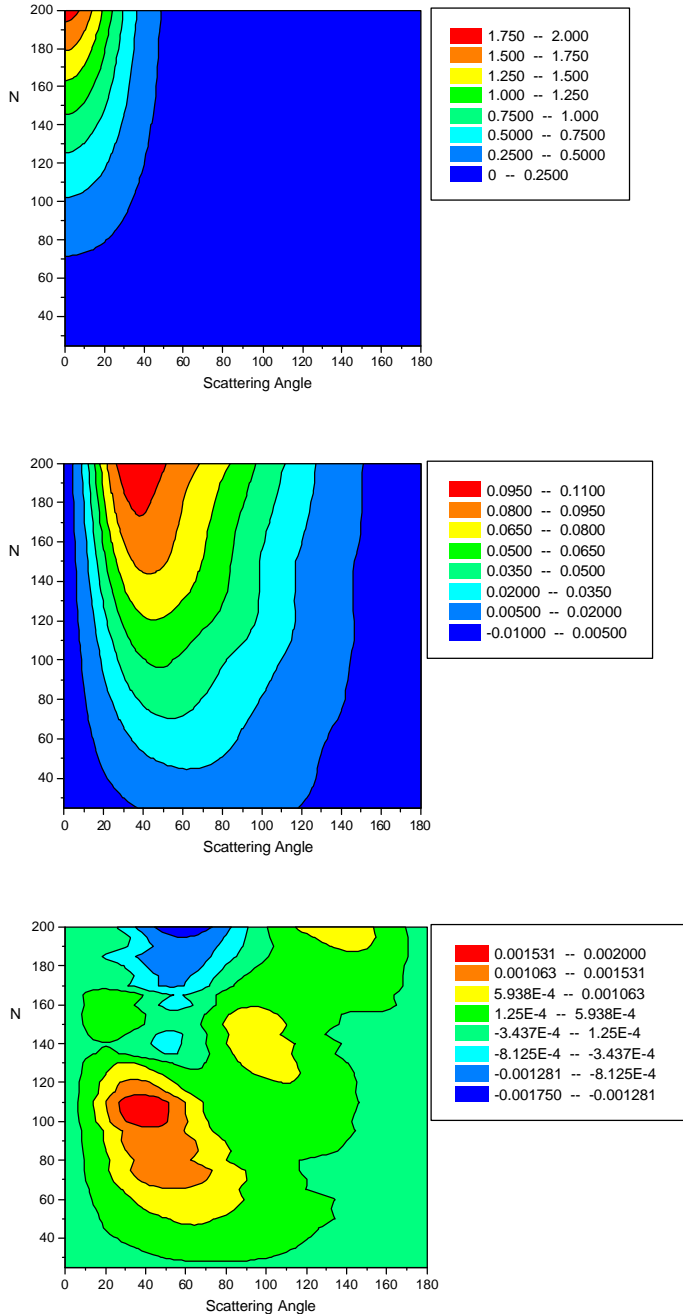


**Fig.4** Angular profiles of  $S_{11}$ ,  $S_{12}$ , and  $S_{34}$  elements, respectively, for different-size soot agglomerates, where number of monomers  $N$  changes between 20 and 200; as calculated by AGGLOME. Fractal dimension is 1.8, the value of the fractal prefactor is 8.0, and the wavelength is 500 nm (from [8]).

In Figure 4, we depict a series of results obtained for fractal-like agglomerates using the algorithm developed in [6]. Here, we present three Mueller matrix elements,  $S_{11}$ ,  $S_{12}$ , and  $S_{34}$ , respectively. These elements dictate the scattering pattern of an object, and if they are determined from experimentally measured scattering signals, they help in characterizing particle shapes and structures.

The first panel in Fig. 4 shows the  $S_{11}$  contours as a function of scattering angle and  $N$ , the number of monomers that make up soot agglomerate [8]. Practically, the  $S_{11}$  is equivalent to the scattering phase function, and it is obvious that the angular scattered-intensity experiments are not likely to yield much information about the structure of fractals. This is more obvious especially when we realize that performing experiments within the forward 10 to 15 degrees is quite difficult, as forward scattered and transmitted components usually difficult to separate. On the other hand, the second and the third panel show clearly that both  $S_{12}$  and  $S_{34}$  have much more detail, and more sensitive to both the  $N$  and the scattering angle.  $S_{12}$  can be considered as a measure of depolarization and  $S_{34}$  stems from the change in the polarization of elliptically polarized light. Measurements of these two terms are possible only if we use polarized light and change its ellipticity systematically [6]

Fractal agglomerate concept discussed in Fig. 4 is applicable to many structures, including soot agglomerates. On the other hand, in material characterization one faces many different shapes and structures, and these shapes may change during the actual fabrication process. To explore the possibility of detecting these structural changes, we have constructed several different shapes, again using the bottom-up procedure (see examples in Fig. 3) and determined their scattering signatures using the dedicated computer programs [6]. In Fig. 5,  $S_{11}$ ,  $S_{12}$ , and  $S_{34}$  profiles are depicted as a function of scattering angle, for an ellipse, a rectangle, a square, and a triangle shaped particles at a wavelength of  $\lambda=632$  nm [9]. Again, we note that the phase function information cannot be used alone to identify the particle structures; however, a combined analysis of all three  $S_{ij}$  profiles will allow us to determine the required shapes. We also note that  $S_{12}$  profiles show that sharp-edged particles depolarize radiation more; i.e., (absolute)  $S_{12}$  values for these particles are larger.

Several other approaches have been considered over the years to determine the  $S_{ij}$  elements for different particle geometries, including coated spheres [10] and multilayer cylinders [11], and recently those of bubbles in a homogeneous media [12,13]. In addition, the discrete-dipole approximation of Draine [14] has been adapted for investigation of agglomerate properties for dependent scattering predictions [15,16] as well as for the interpretation of sooty diffusion flames [17,18]. These models, as well as those available from the literature [5], are likely to provide an extensive database for interpretation of future experimental data.

## EXPERIMENTAL RESULTS

In order to detect the fine structural variations of small particles and agglomerates we discussed above, we have developed several nephelometers over the years and the concept was continually improved [6,8,9,19-24]. In most recent attempts, we used elliptically polarized light, where first we had to determine six unique sets of retarder and polarizer settings to

make six different and accurate scattering measurements [6,23]. These unique settings are pre-determined following a series of numerical experiments using the available algorithms. After that, the six  $S_{ij}$  elements,  $S_{11}$ ,  $S_{12}$ ,  $S_{22}$ ,  $S_{33}$ ,  $S_{44}$ ,  $S_{34}$  are recovered from the recorded intensities in a numerical inverse analysis.

Figure 6 depicts the latest version of the elliptic nephelometer, which is discussed in Aslan et al. [24]. These types of equipment are usually calibrated with particles of known properties. In this case, the system was designed for detection of cotton-fiber properties. For that reason, we tested the system using quartz fibers. The detailed results of these experiments are shown in Fig. 7, where the data for a single

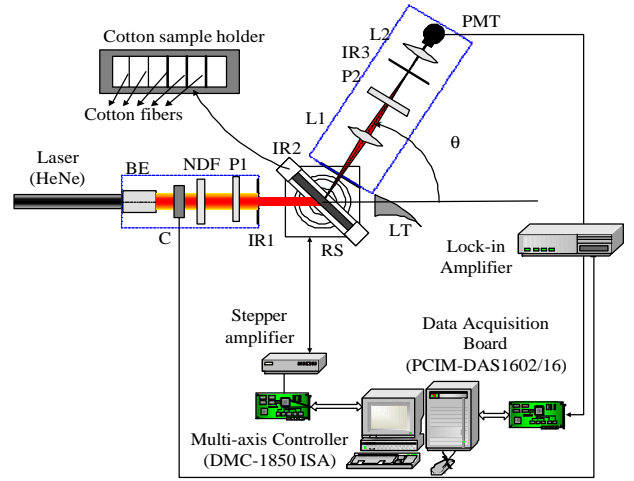


**Fig.6** Schematic of the experimental nephelometer used for cotton-fiber experiments. L: Lens; P: Polarizer; BE: Beam expander; NDF: Neutral density filter; PMT: Photo-multiplier tube; IR: Iris; RS: Rotary scale. [24].

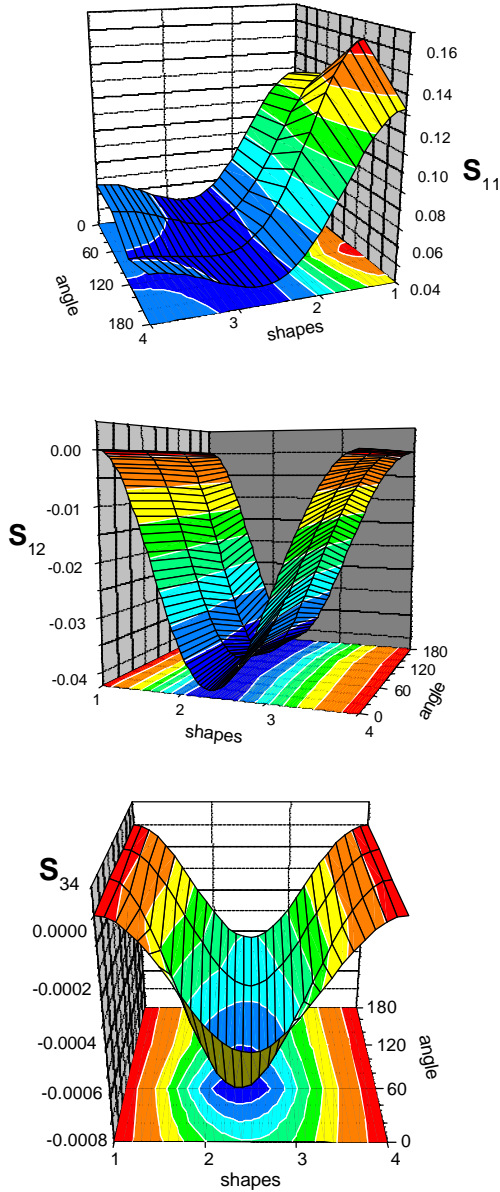


**Fig.5** Angular profiles of  $S_{11}$ ,  $S_{12}$ , and  $S_{34}$  elements for different structures: 1: ellipse, 2: rectangle, 3: square, 4: triangle [9].

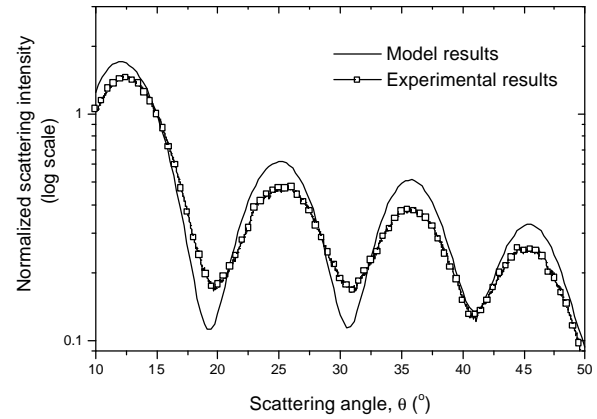


**Fig. 7** Results of calibration experiments: the Lorenz-Mie predictions are compared against the experimental data obtained for circular cylinders: cylinder diameter:  $4.005 \mu\text{m}$ ; the quartz index of refraction of  $m=1.457-i0$ ,  $\lambda=532 \text{ nm}$ . [24].

quartz fiber are compared against the Lorenz-Mie predictions for cylindrical fibers. The agreement is near perfect for all elements, even though only  $S_{11}$  is shown here.

The system was later used to detect the scattering patterns of convoluted cotton-fibers and the data were compared against a finite element method developed by Jun Yamada (see [24]). Figure 8 shows that the agreement is quite satisfactory. These experiments allowed us to establish a relationship between scattering signals and the cotton fineness and maturity [24].

The same system was later modified and used for detection of various metallic nano-particles. These types of particles are usually difficult to model, as they have large imaginary components of the refractive index, and they tend to agglomerate. Figure 9 depicts the TEM images of three different particles considered in the experiments. And finally, Fig. 10 shows the normalized  $S_{22}$  profiles recovered from

extensive experiments [25] and the comparisons against the numerical models. These results clearly show that the particles are not spherical, and agglomeration can be predicted effectively using Chebyshev polynomials. More detailed numerical studies are currently being carried out in our laboratory. It is obvious that by such shape characterization, a material fabrication process can be better understood and improved to achieve the desired structures and size distributions.

## SUMMARY

In this paper, an outline of our on-going particle characterization research is presented. Even though we believe that the elliptically-polarized light scattering approach we have developed over the years is a robust and accurate characterization technique for fine particles, by no means we claim that this is the only approach available. Neither have we claimed that this paper is an exclusive review of the literature. However, in each paper we referred, the reader will find more detailed and relevant review of the literature.

This approach can be extended to nano-structures if the novel experimental tools can be developed, which is our current research focus.

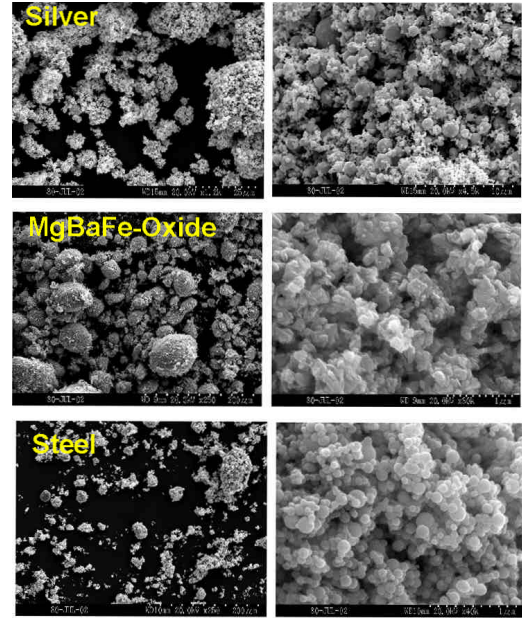


**Fig. 9** TEM pictures for three different metallic particles: For Silver, the scale is 25  $\mu\text{m}$  (left) and 10  $\mu\text{m}$  (right); for the others, it is 250  $\mu\text{m}$  (left) and 1  $\mu\text{m}$  (right). [25].

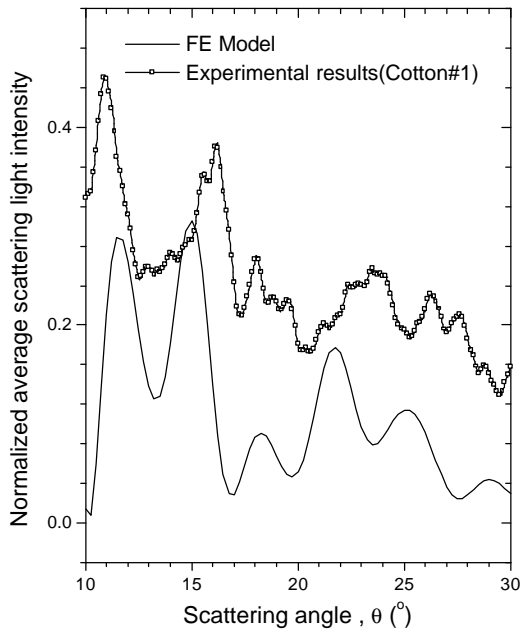


**Fig. 8** Comparisons of single cotton-fiber experiments with the finite element model predictions. Only the phase function profiles are shown. [24].

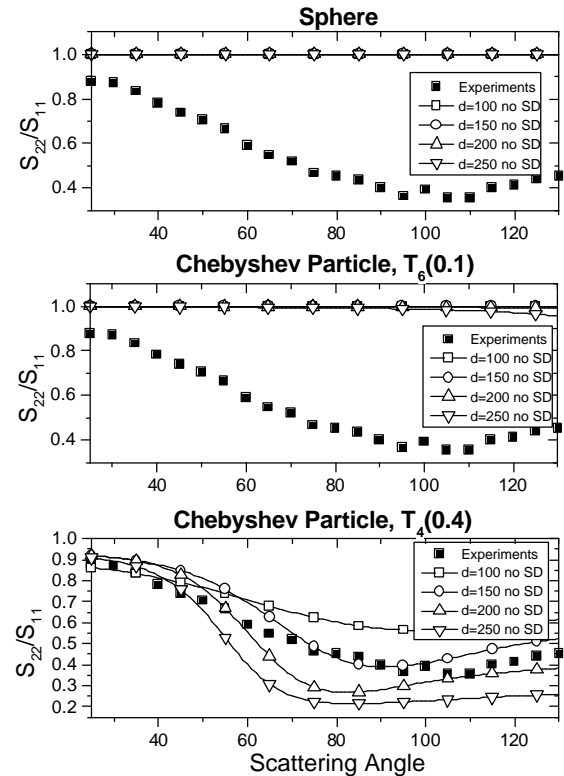


**Fig. 10** Normalized  $S_{22}$  profiles measured for the metallic structures shown in Fig. 9. Match with Chebyshev  $T_4(0.4)$  particles show that particles are not spherical in shape and about 150 nm in average size (effective diameter) [25].

## ACKNOWLEDGMENTS

The particle characterization research at the University of Kentucky has been sponsored over the years by NSF, DOE-PETC, TRW, ENEL-Italy, CNR Istituto Motori-Italy, USDA-NIR, and Synergetic Technologies Inc. Contributions of Dr. S. Manickavasagam, Dr. M. Aslan, Mr. B. Wong and Mr. R. Govindan to different aspects of this research have been significant. Without the help of former and graduate students, including, in alphabetical order, B. Agarwal, S. Alstedt, D. Bhandi, C. Crofcheck, D. Dsa, P. Dutta, S. Ghosal, Z. Ivezic, C. Klusek, M. Kozan, A. Mahadeviah, D.-K. Qing, and S. Subramaniam, this work could not be carried out. Finally, Dr. C. Saliel of the STI, along with Dr. S. Manickavasagam, had tremendous contribution to the development of the final, easy-to-use version of the instrument [26]. The author gratefully acknowledges their professional efforts to this endeavor.

## REFERENCES

- [1] R. Viskanta and M.P. Mengüç, "Radiative Heat Transfer in Combustion Systems," *Progress in Energy and Combustion Sciences*, Vol. 13, pp. 97-160, 1987.
- [2] M.F. Modest, Radiative Heat Transfer, McGraw-Hill, New York, 1993.
- [3] J.R. Howell and M.P. Mengüç, "Radiation," in *Handbook of Heat Transfer*, Chapter 7, Editors: W. Rohsenow, J. Hartnett, Y. Cho, McGraw Hill, 1998.
- [4] C. F. Bohren and D.R. Huffman, *Absorption and Scattering of Light by Small Particles*, John Wiley & Sons, New York, 1983.
- [5] M. I. Mishchenko, J.W. Hovenier, L.D. Travis, *Light Scattering by Nonspherical Particles*, Academic Press, New York, 2000.
- [6] S. Manickavasagam and M.P. Mengüç, "Scattering Matrix Elements of Fractal-like Soot Agglomerates," *Applied Optics*, Vol. 36, No. 6, pp. 1337-1351, 1997.
- [7] M.P. Mengüç and S. Manickavasagam, "Radiation Transfer and Polarized Light," *International Journal of Engineering Sciences*, Special issue on memory of S. Chandrasekhar, Vol. 36, pp. 1569-1593, 1998.
- [8] C. Klusek, S. Manickavasagam and M.P. Mengüç, "Compendium of Scattering Matrix Elements for Soot Agglomerates," *Journal of Quantitative Spectroscopy and Radiative Transfer*, 2003 (in press)
- [9] M. Kozan, M.P. Mengüç, S. Manickavasagam, C. Saliel, "Effect of Particle Shape Irregularities on the Angular Profiles of Scattering Matrix Elements," 8<sup>th</sup> Joint AIAA/ASME Thermophysics and Heat Transfer Conference, St. Louis, MO, June 24-26, 2002.
- [10] D. Bhandi, S. Manickavasagam, and M.P. Mengüç, "Identification of Non-Homogeneous Spherical Particles from their Scattering Matrix Elements," *Journal of Quantitative Spectroscopy and Radiative Transfer*, Vol. 56, No. 4, pp. 591-608, 1996.
- [11] S. Manickavasagam and M.P. Mengüç, "Scattering Matrix Elements of Coated Infinite-Length Cylinders," *Applied Optics*, Vol. 37, No. 12, pp. 2473-2482, 1998.
- [12] B. Wong and M.P. Mengüç, "Depolarization of Radiation by Foams," *JQSRT*, Vol. 73, Numbers 2-5, pp. 273-284, 2002.
- [13] B. Wong, R. Vaillon and M.P. Mengüç, "Propagation of Polarized Light in Foamy Materials: A Vector Monte Carlo Approach via Stokes Parameters," (to be presented at the ASME/IMECE) 2003.
- [14] B. Draine, "The Discrete-Dipole Approximation and its Application to Interstellar Graphite Grains," *Astrophysics J.* Vol. 333, pp. 848-872, 1988.
- [15] Z. Ivezic and M.P. Mengüç, "An Investigation of Dependent-Independent Scattering Regimes for Soot Particles Using Discrete Dipole Approximation," *International Journal of Heat and Mass Transfer*, Vol. 39, No. 7, pp. 811-822, 1996.
- [16] Z. Ivezic, M.P. Mengüç, and T.G. Knauer, "A Procedure to Determine the Onset of Soot Agglomeration from Multiwavelength Experiments," *Journal of Quantitative Spectroscopy and Radiative Transfer*, Vol. 57, No. 6, pp. 859-865, 1997.
- [17] M.P. Mengüç, A. Mahadeviah, K. Saito, S. Manickavasagam, "Application of the Discrete Dipole Approximation to Determine the Radiative Properties of Soot Agglomerates," in Heat Transfer in Fire and Combustion Systems; ASME HTD-Vol. 199, pp. 9-16, August, 1992.
- [18] B. M. Vaglieco, O. Monda, F. E. Corcione, M. P. Mengüç, "Optical and Radiative Properties of Particulates at Diesel Engine Exhaust," *Combustion Science and Technology*, Vol. 102, pp. 283-299, 1994.
- [19] B.M. Agarwal and M.P. Mengüç, "Single and Multiple Scattering of Collimated Radiation in an Axisymmetric System," *International Journal of Heat and Mass Transfer*, Vol. 34, No. 3, pp. 633-647, 1991.
- [20] S. Manickavasagam and M.P. Mengüç, "Effective Optical and Radiative Properties of Coal Particles as Determined from FT-IR Spectroscopy Experiments," *Energy and Fuel*, Vol. 7, No. 6, pp. 860-869, 1993.
- [21] M.P. Mengüç, S. Manickavasagam, and D.A. D'sa, "Determination of Radiative Properties of Pulverized Coal Particles from Experiments," *FUEL*, Vol. 73, No. 4, pp. 613-625, 1994.
- [22] M.P. Mengüç and P. Dutta, "Scattering Tomography and Application to Sooting Diffusion Flames," *ASME Journal of Heat Transfer*, Vol. 116, No. 1, pp. 144-151, 1994.
- [23] R. Govindan, S. Manickavasagam, and M.P. Mengüç, "On Measuring the Mueller Matrix Elements of Soot Agglomerates," Radiation-I: Proceedings of the First International Symposium on Radiative Heat Transfer; presented at Kusadasi, Turkey, August 1995. Begell House, NY, 1996.
- [24] Aslan, M., Yamada, J., Mengüç, M.P., Thomasson, A., "Radiative Properties of Individual Cotton Fibers: Experiments and Predictions," *AIAA Journal of Thermophysics and Heat Transfer* (2003) (in press).
- [25] Aslan, M., Mengüç, M.P., "Experimental Measurements of Scattering Matrix Elements of Colloidal Metallic Ultrafine Particles," (in preparation) (2003).
- [26] S. Manickavasagam, M. P. Mengüç, Z. B. Drozdowicz, C. Ball, "Size, Shape, and Structure Analysis of Fine Particles," *American Ceramic Society Bulletin*, July 2002. (ACSB is a Trade Magazine).